J BONE ONCOL 51 (2025) 100670

Contents lists available at ScienceDirect

Journal of Bone Oncology

journal homepage: www.elsevier.com/locate/jbo

Research Paper

Impact of myosteatosis on prognosis in multiple myeloma patients: A subgroup analysis of 182 cases and development of a nomogram☆

Jun-Peng Liu [a,1], Xing-Chen Yao [a,1], Ming Shi [a,1], Zi-Yu Xu [a], Yue Wu [a], Xiang-Jun Shi [b], Meng Li [a], Xin-Ru Du [a,*]

[a] Department of Orthopaedic Surgery, Beijing Chaoyang Hospital, Capital Medical University, Beijing 100020, China
[b] Department of Rheumatology, Beijing Tiantan Hospital, Capital Medical University, Beijing 100020, China

HIGHLIGHTS

- Myosteatosis demonstrated no significant association with survival outcomes in MM patients.
- Severe myosteatosis increases fracture risk and back pain in early-stage MM.
- FIR fracture prediction weakens in MM with BMI ≥25 kg/m^2 or RBC >3.68×10^{12}/L.
- Age, BMI, gender, RBC predict myosteatosis; validated nomogram developed.

ARTICLE INFO

Keywords:
Multiple myeloma
Myosteatosis
Paravertebral muscle
Fatty infiltration rate
Fracture
Nomogram

ABSTRACT

Background: This study aims to explore the prognostic value of myosteatosis in multiple myeloma (MM) and to analyze the factors influencing myosteatosis.

Methods: A retrospective analysis was conducted on 182 patients treated for MM at our institution from 2009 to 2020 who underwent MRI examinations. The fatty infiltration rate (FIR) of the erector spinae and multifidus muscles at the L3 level was measured to assess the degree of myosteatosis. Patients were grouped based on fracture presence and median FIR, and group differences were compared, with $P < 0.05$ considered statistically significant. Survival and fractures were used as prognostic indicators, and regression analysis was performed to determine the impact of FIR on these outcomes in MM patients. The factors influencing FIR were analyzed, and the relationship between myosteatosis and MM prognosis was further analyzed within its sensitive subgroups. Finally, a nomogram based on FIR was established and validated.

Results: Significant differences were observed between the fracture and non-fracture groups in lactate dehydrogenase, serum phosphorus, visual analogue scale, oswestry disability index and FIR ($P < 0.05$). When patients were grouped based on the median FIR (28.89 %), there were significant differences in age, sex, body mass index (BMI), red blood cell (RBC) count, hemoglobin, hematocrit, albumin, visual analogue scale, oswestry disability index, and fracture incidence ($P < 0.05$). Univariate COX regression analysis indicated that myosteatosis had no significant impact on survival prognosis in MM patients ($HR = 0.999$, $P = 0.852$), with a log-rank test P value of 0.11 when grouped by the cut-off FIR value of 33.67 %. Multivariate logistic regression indicated that FIR is an independent predictor of fractures ($OR = 1.054$, $P = 0.000$). Multivariate linear regression revealed that age, sex, RBC count, and BMI are independent factors influencing FIR ($P < 0.05$). When not grouped, FIR's prediction of

Abbreviations: MM, Multiple myeloma; FIR, Fat infiltration rate; ISS, International Staging System; DS, Durie-Salmon; Ig, Immunoglobulin; BMI, Body Mass Index; WBC, White Blood Cell count; PLT, Platelet count; RBC, Red Blood Cell count; Hb, Hemoglobin; HCT, Hematocrit; ALB, Albumin; BUN, Blood Urea Nitrogen; CREA, Creatinine; γ-GT, Gamma-Glutamyl Transferase; ALT, Alanine Aminotransferase; AST, Aspartate Aminotransferase; ALP, Alkaline Phosphatase; LDH, Lactate Dehydrogenase; Serum β2MG, Serum Beta-2 Microglobulin; CRP, C-Reactive Protein; BNP, B-type Natriuretic Peptide; VAS, Visual Analog Scale; ODI, Oswestry Disability Index; PM, psoas major muscle; QL, quadratus lumborum muscle; ES, erector spinae muscles; MF, multifidus muscle; ROC, Receiver Operating Characteristic; AUC, Area Under the ROC Curve; DCA, Decision Curve Analysis; CIC, Clinical Impact Curve.

☆ This article is part of a special issue entitled: 'Myeloma bone disease' published in Journal of Bone Oncology.

* Corresponding author.
E-mail address: duxinru@163.com (X.-R. Du).

[1] Contribute equally.

https://doi.org/10.1016/j.jbo.2025.100670
Received 29 December 2024; Received in revised form 24 February 2025; Accepted 2 March 2025
Available online 11 March 2025

fractures showed no significant interaction with age, sex, RBC count, or BMI (P for interaction > 0.05). In subgroups with BMI ≥ 25 kg/m^2 or RBC count > 3.68 × 10^12/L, FIR lost its predictive significance for fractures. The FIR nomogram model had a C-index of 0.777, and the calibration curve, decision curve analysis, and clinical impact curve all validated its effectiveness.

Conclusions: Myosteatosis characterized by FIR is not a reliable predictor of survival in MM patients but is effective in predicting fractures and is closely related to back pain and functional impairment. FIR is significantly associated with age, sex, RBC count, and BMI.

1. Introduction

Multiple myeloma (MM) is the second most common hematologic malignancy, with an annual incidence rate of up to 5 per 100,000 people [1], accounting for approximately 20 % of total deaths from hematologic malignancies [2]. Therefore, survival status is a crucial measure of prognosis in MM patients [1]. As treatment regimens have evolved, the survival time of MM patients has increased, highlighting the need for greater focus on the assessment and improvement of patients' quality of life. Bone destruction is a hallmark of MM [3], with about 80 % of patients suffering from bone disease and 90 % experiencing low back pain [4], significantly impacting daily life.

Myosteatosis is defined as increased fat infiltration in skeletal muscle, which negatively affects muscle mass, strength, mobility, and normal metabolism by changing muscle fiber orientation [5]. Recent studies have linked myosteatosis to poor disease prognosis [6,7], making its impact and underlying mechanisms a hot topic. In the field of MM, several studies have explored the relationship between myosteatosis and survival outcomes in MM patients. However, the results have been inconsistent and sometimes even contradictory [8,9]. Therefore, further investigation into the association between myosteatosis and survival prognosis in MM patients, based on the data from our institution, is of significant importance. Additionally, bone disease is a hallmark feature of MM, yet there is currently limited evidence regarding the relationship between fractures and the degree of myosteatosis in MM patients. Thus, exploring the correlation between myosteatosis and fractures is another key focus of this study.

The lumbar, particularly the third lumbar vertebra (L3), which serves as the mechanical center, is prone to degeneration due to its high mobility and load-bearing function [10]. Among the lumbar muscles, the multifidus and erector spinae are most closely linked to the body's overall condition [11]. Based on this information, our study measured the fat infiltration rate (FIR) of the erector spinae and multifidus muscles at the L3 level in MM patients to assess the extent of myosteatosis [12,13].

The objectives of this study are as follows: (1) To analyze the relationship between myosteatosis and survival prognosis in MM patients; (2) To clarify the relationship between myosteatosis and lumbar fractures, low back pain, and lumbar function in MM patients; (3) To validate the relationship between myosteatosis and prognosis in sensitive subgroups of MM patients; and (4) To analyze the factors influencing FIR, establish and validate a predictive model to guide clinicians in identifying risk factors for myosteatosis, enabling timely prevention and intervention measures to improve the clinical prognosis and quality of life of MM patients.

2. Methods

2.1. Study design

We retrospectively reviewed the records of patients treated for MM at our institution from 2009 to 2020. All patients were treated by the same medical team. The study received approval from our institutional ethics committee (Ethics Approval No. 2023-ke-394). Upon hospital admission, all patients underwent routine lumbar MRI scans, regardless of their disease severity or symptoms. The study start date was defined as the date of the patient's first MRI. Follow-up information was obtained through outpatient visits or telephone interviews, with the last follow-up conducted in December 2023.

2.2. Inclusion and exclusion criteria

Inclusion criteria: (1) Age ≥ 18 years; (2) Newly diagnosed MM patients who fulfill the diagnostic criteria of the International Myeloma Working Group (IMWG); (3) Complete follow-up data. Exclusion criteria: (1) Patients who used bone-affecting drugs such as bortezomib, bisphosphonates, or corticosteroids prior to the MRI scan; (2) Presence of other conditions that could affect muscle FIR, such as thyroid disease; (3) History of lumbar spine disease or surgery; (4) Severe bone disease or osteoporosis; (5) Death, fracture, or lumbar symptoms due to non-MM events.

2.3. Data collection

Data collected included the patient's age, sex, International Staging System (ISS) stage, Durie-Salmon (DS) stage, isotype, body mass index (BMI), white blood cell (WBC) count, platelet (PLT) count, red blood cell (RBC) count, hemoglobin (Hb), hematocrit (HCT), albumin (ALB), blood urea nitrogen (BUN), creatinine (CREA), gamma-glutamyl transferase (γ-GT), alanine aminotransferase (ALT), aspartate aminotransferase (AST), alkaline phosphatase (ALP), lactate dehydrogenase (LDH), serum beta-2 microglobulin (β2MG), C-reactive protein (CRP), B-type natriuretic peptide (BNP), serum phosphorus, serum calcium, proportion of bone marrow plasma cells, serum M−protein, and FIR. We also recorded the patient's Visual Analogue Scale (VAS) and Oswestry Disability Index (ODI) scores at the time of MRI. The survival data of the patients during the follow-up period and the occurrence of lumbar fractures within three years after completing the MRI examination were recorded.

2.4. Evaluation of myosteatosis

Routine diagnostic MRI of the lumbar spine was performed using a 1.5-T MR system (Siemens Magnetom Avanto, Siemens Healthineers, Erlangen, Germany). The subjects were positioned in the supine position with the lumbar spine in a neutral posture, and a pillow was placed under the knees. Images were acquired at the intervertebral disc level using the same T2-weighted fast spin-echo pulse sequence [14]. FIR was measured using Image J (NIH, Bethesda, MD, USA). Based on the European Working Group on Sarcopenia in Older People standards [15], DICOM images of the L3 level from T2-weighted axial MRI scans were used. Four 30 mm^2 regions were evenly drawn in the subcutaneous fat areas, 2 cm lateral to the posterior midline on both sides and 4 cm lateral to the transverse process at the L3 level. The signal intensity was measured, and the 5 %–95 % range of the signal intensity was defined as the fat tissue signal range [6,13]. The fascial boundaries of the erector spinae and multifidus muscles [12] were manually outlined to determine the region of interest (Fig. 1***A***) [16]. Using the threshold tool, fat tissue within the region of interest was highlighted in red, and the percentage of fatinfiltrated area was measured using a pseudocoloring technique (Fig. 1***B***), with the average of both sides taken as the result. All images were measured independently by two experienced doctors, one specializing in orthopedics and the other in radiology, each with

over five years of musculoskeletal imaging diagnostic experience. The reliability of measurements between the two independent recorders was assessed using Pearsons' correlation coefficient, yielding correlation coefficient (r) of 0.945 (P = 0.000), indicating high consistency. The average of the measurement results was taken as the final result.

2.5. Statistical analysis

Data were analyzed using IBM SPSS 25.0 (IBM Corp, Armonk, NY, USA). The Kolmogorov-Smirnov test was used to determine the normality of variables. Continuous data following a normal distribution were expressed as mean ± standard deviation ($\bar{x}\pm s$), non-normal data as median [first quartile; third quartile], and enumeration data as frequency (n, %). The median survival time was calculated using Kaplan-Meier survival curves. Patients were grouped based on the presence of fractures and the median FIR, and differences between groups were compared. The independent samples *t*-test was used for normally distributed data, and the Mann-Whitney *U* test was used for skewed data and ordinal data. Unordered categorical data were analyzed using the Chi-square test: Pearson Chi-Square for Expected Counts > 5, Fisher' s Exact Test for Expected Counts < 1, and Likelihood Ratio for intermediate values. A P-value (two-tailed) < 0.05 was considered statistically significant.

The relationship between FIR and patient survival prognosis was analyzed using univariate COX regression. The FIR cut-off value was calculated using the "survminer" package in R Studio 4.2.1 (R Development Core Team, Vienna, Austria). The cut-off value was used to group patients, and survival curves were plotted using the "ggsurvplot" package with log-rank tests performed. The relationship between FIR and lumbar fractures was analyzed using univariate logistic regression. Due to the exploratory nature of this analysis, variables with P < 0.1 from univariate logistic regression, along with those showing P < 0.05 in group comparisons, were included in multivariate logistic regression. Dummy variables were set for unordered categorical data, ensuring correlation coefficients <0.5, tolerance >0.1, and variance inflation factor <5. Independent fracture risk factors were identified using Forward LR with P < 0.05. The Receiver Operating Characteristic (ROC) curve was plotted to evaluate model discrimination, and the area under the ROC curve (AUC) was used to assess model performance. AUC or C-index values range from 0.5 (random probability) to 1.0 (perfect fit), with values >0.7 generally indicating good model performance. The cut-off value corresponding to the maximum Youden index was calculated.

Univariate linear regression was conducted with FIR as the dependent variable. Variables with P < 0.1, as well as those showing significant differences in FIR grouping (P < 0.05), were included in multivariate linear regression. Independent influencing factors were identified using stepwise regression with P < 0.05. ROC curves were plotted using IBM SPSS 25.0, and the AUC and cut-off values for each independent FIR influencing factor were calculated. Continuous variables among FIR's independent influencing factors were converted into binary variables using appropriate cut-off points. Subgroup analysis was performed, and forest plots were drawn using the "jstable" and "forestploter" packages in R Studio 4.2.1. P for interaction <0.05 was considered statistically significant, indicating that FIR's predictive performance for outcome events varied across the corresponding subgroups.

A nomogram model based on FIR regression results was developed using the "rms" package in R Studio 4.2.1. ROC curves were plotted using the "pROC" package, and the C-index and 95 % confidence intervals were calculated to assess model discrimination. Internal validation was performed using the bootstrap method (1,000 times), and calibration curves were plotted to evaluate model calibration. A close fit between the curve and the 45° diagonal line indicated that the predicted probability closely matched the actual results. The Decision Curve Analysis (DCA) and Clinical Impact Curve (CIC) based on a population size of 1,000 were generated using the "rmda" package to evaluate the clinical impact of the predictive model.

3. Results

3.1. General information

Based on the inclusion and exclusion criteria, a total of 182 patients were included in the study (Table 1). The median follow-up period was 53 months. During the follow-up, 79 patients (43.41 %) died, with a median survival time of 68 months (Fig. 2***A***), 95 % CI (47.246, 88.754). The average disease duration at the time of MRI was 4.2 months (range: 1–6 months). Within three years following the initial MRI examination, 80 patients (43.96 %) developed lumbar fractures. There were statistically significant differences between patients with and without fractures in terms of LDH, serum phosphorus, VAS, ODI, and FIR (P < 0.05, Table 1). The mean FIR of the patients was 33.30 % and the median FIR was 28.89 % [20.11 %, 39.53 %]. The average FIR for patients who experienced fractures was 41.68 %, while the average FIR for patients who did not experience fractures was 26.74 %. There were statistically significant differences in age, sex, BMI, RBC, Hb, HCT, ALB, VAS, ODI, and fracture incidence between the FIR Low and FIR High groups (P < 0.05, Table 1).

3.2. Clinical significance of myosteatosis

Using the survival data of 182 patients as the dependent variable and

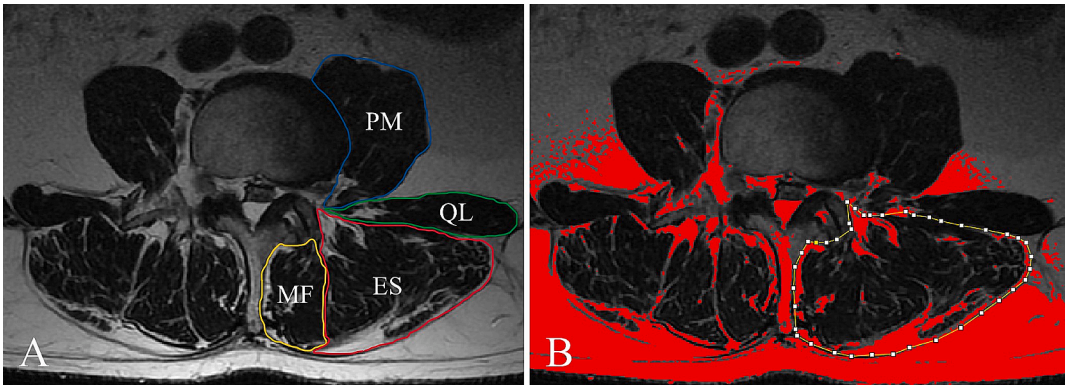

Fig. 1. MRI at the L3 level (A) Schematic diagram of lumbar muscle anatomy. PM, psoas major muscle; QL, quadratus lumborum muscle; ES, erector spinae muscles; MF, multifidus muscle (B) Using ImageJ to convert DICOM images to 8-bit type, with subcutaneous fat signal as the reference range for intramuscular fat signal, manually delineate the region of interest. Then, use the Threshold tool to highlight the fat within the region in red. (For interpretation of the references to colour in this figure legend, the reader is referred to the web version of this article.)

Table 1
The general information of patients (n = 182).

Parameters	Total (n = 182)	Fracture			Fat infiltration rate		
		No (n = 102)	Yes (n = 80)	P	Low (n = 91)	High (n = 91)	P
Fat infiltration rate (%)	33.30 ± 18.91	26.74 ± 12.55	41.68 ± 22.16	< 0.001*	——	——	——
Age (years)	58.58 ± 9.99	57.94 ± 10.41	59.40 ± 9.44	0.330	55.66 ± 9.15	61.51 ± 9.99	<0.001*
Sex				0.654			0.001*
Male	93 (51.1 %)	54(52.9 %)	39(48.8 %)		58(63.7 %)	35(38.5 %)	
Female	89(48.9 %)	48(47.1 %)	41(51.2 %)		33(36.3 %)	56(61.5 %)	
ISS stage				0.092			0.246
I	40(22.0 %)	28(27.5 %)	12(15.0 %)		24(26.4 %)	16(17.6 %)	
II	101 (55.5 %)	53(52.0 %)	48(60.0 %)		50(54.9 %)	51(56.0 %)	
III	41(22.5 %)	21(20.6 %)	20(25.0 %)		17(18.7 %)	24(26.4 %)	
DS stage				0.288			0.610
I	6 (3.3 %)	3(2.9 %)	3(3.8 %)		4(4.4 %)	2(2.2 %)	
II	18 (9.9 %)	13(12.7)	5(6.3 %)		10(11.0 %)	8(8.8 %)	
III	158 (86.8 %)	86(84.3 %)	72(90.0 %)		77(84.6 %)	81(89.0 %)	
Isotype				0.573			0.206
IgG	96 (52.7 %)	59 (57.8 %)	37 (46.3 %)		47 (51.65 %)	49 (53.85 %)	
IgA	32 (17.6 %)	15 (14.7 %)	17 (21.3 %)		17 (18.68 %)	15 (16.48 %)	
Light chain	31 (17.0 %)	13 (12.7)	18 (22.5 %)		13 (14.29 %)	18 (19.78 %)	
IgD	18 (9.9 %)	12 (11.8 %)	6 (7.5 %)		11 (12.09 %)	7 (7.69 %)	
Nonsecretory	4 (2.2 %)	3 (2.9 %)	1 (1.3 %)		3 (3.30 %)	1 (1.10 %)	
Double M	1 (0.5 %)	0	1 (1.3 %)		0	1 (1.10 %)	
BMI (kg/m^2)	24.07 ± 3.25	23.85 ± 3.46	24.35 ± 2.95	0.313	23.61 ± 3.16	24.56 ± 3.29	0.049*
WBC (×10^9/L)	5.24 ± 2.47	5.37 ± 2.58	5.06 ± 2.34	0.395	5.19 ± 2.28	5.28 ± 2.67	0.822
PLT (×10^9/L)	173.19 ± 89.55	174.85 ± 98.73	171.07 ± 76.83	0.778	179.98 ± 98.67	166.41 ± 79.37	0.308
RBC (×10^12/L)	3.19 ± 0.88	3.21 ± 0.93	3.16 ± 0.81	0.727	3.42 ± 0.92	2.95 ± 0.77	<0.001*
Hb (g/L)	99.18 ± 26.14	99.92 ± 27.81	98.24 ± 23.98	0.667	106.27 ± 27.46	92.09 ± 22.76	< 0.001*
HCT (%)	30.04 ± 7.55	30.39 ± 8.01	29.60 ± 6.93	0.481	31.93 ± 7.83	28.15 ± 6.78	0.001*
ALB (g/L)	31.71 ± 6.69	31.28 ± 6.47	32.26 ± 6.96	0.328	32.97 ± 6.23	30.45 ± 6.92	0.011*
BUN (mmol/L)	7.00 ± 4.97	6.84 ± 4.41	7.20 ± 5.63	0.628	6.34 ± 3.58	7.66 ± 6.01	0.074
CREA (μmoI/L)	76.45 [59.58, 100.53]	80.25[59.50,107.60]	72.10[59.73,90.08]	0.234	81.20[61.20, 99.60]	72.00[57.40, 104.30]	0.333
γ-GT (U/L)	28.00 [19.00, 45.00]	30.00[21.00, 46.00]	25.00[17.25,42.25]	0.547	28.00[20.00, 48.50]	28.00[17.75, 44.50]	0.899
ALT(U/L)	22.35 ± 14.28	22.78 ± 17.36	21.80 ± 9.21	0.803	21.69 ± 11.50	23.01 ± 17.06	0.737
AST(U/L)	23.15 ± 12.61	24.07 ± 14.40	21.98 ± 10.02	0.544	22.30 ± 10.17	24.00 ± 15.04	0.624
ALP(U/L)	91.41 ± 52.64	89.65 ± 44.54	93.65 ± 61.68	0.612	87.05 ± 44.32	95.76 ± 59.75	0.266
LDH (U/L)	150.00[128.00, 182.00]	145.00[128.25,166.50]	160.50[127.25, 205.75]	0.045*	149.00[125.00, 181.00]	150.00[130.00, 193.00]	0.523
Serum β2MG (mg/L)	3.16[2.27, 4.71]	3.18[2.27,4.87]	3.14[2.25,4.49]	0.970	3.00[2.27, 4.12]	3.84[2.18, 5.09]	0.148
CRP (mg/L)	0.42[0.21, 0.96]	0.43[0.18,1.16]	0.41[0.22,0.83]	0.766	0.38[0.18, 0.95]	0.45[0.22, 1.12]	0.114
BNP (pg/ml)	195.95[105.20, 394.25]	217.60[90.39,1336.00]	189.10[110.65,250.85]	0.395	152.50[72.80, 362.75]	204.55[147.60, 457.65]	0.191
Serum phosphorus (mmol/L)	1.28 ± 0.30	1.24 ± 0.35	1.32 ± 0.23	0.049*	1.25 ± 0.26	1.30 ± 0.34	0.215
Serum calcium (mmol/L)	2.15 ± 0.24	2.14 ± 0.25	2.16 ± 0.23	0.544	2.15 ± 0.20	2.15 ± 0.28	0.889
Proportion of bone marrow plasma cells (%)	34.00 ± 23.54	31.47 ± 24.39	37.23 ± 22.18	0.226	32.40 ± 22.06	35.60 ± 25.07	0.497
Serum M−protein (g/L)	53.74 ± 28.99	57.49 ± 29.23	48.96 ± 28.45	0.220	49.45 ± 28.63	58.03 ± 29.10	0.215
VAS	0 [0, 4]	0 [0, 3]	0 [0, 5]	0.005*	0 [0, 3]	0 [0, 5]	< 0.001*
ODI (%)	19.67 ± 10.53	18.28 ± 10.07	21.44 ± 10.96	0.045*	16.55 ± 10.12	22.79 ± 10.80	<0.001*
Fracture				——			<0.001*
Yes	80 (43.96 %)	——	——		25(27.5 %)	55(60.4 %)	
No	102 (56.04 %)	——	——		66(72.5 %)	36(39.6 %)	

Continuous data following a normal distribution were expressed as $\bar{x} \pm s$, non-normal data as median [first quartile; third quartile], and enumeration data as frequency (n, %). *, $P < 0.05$.
ISS, International Staging System; DS, Durie-Salmon; Ig, Immunoglobulin; BMI, Body Mass Index; WBC, White Blood Cell count; PLT, Platelet count; RBC, Red Blood Cell count; Hb, Hemoglobin; HCT, Hematocrit; ALB, Albumin; BUN, Blood Urea Nitrogen; CREA, Creatinine; γ-GT, Gamma-Glutamyl Transferase; ALT, Alanine Aminotransferase; AST, Aspartate Aminotransferase; ALP, Alkaline Phosphatase; LDH, Lactate Dehydrogenase; Serum β2MG, Serum Beta-2 Microglobulin; CRP, C-Reactive Protein; BNP, B-type Natriuretic Peptide; VAS, Visual Analog Scale; ODI, Oswestry Disability Index.

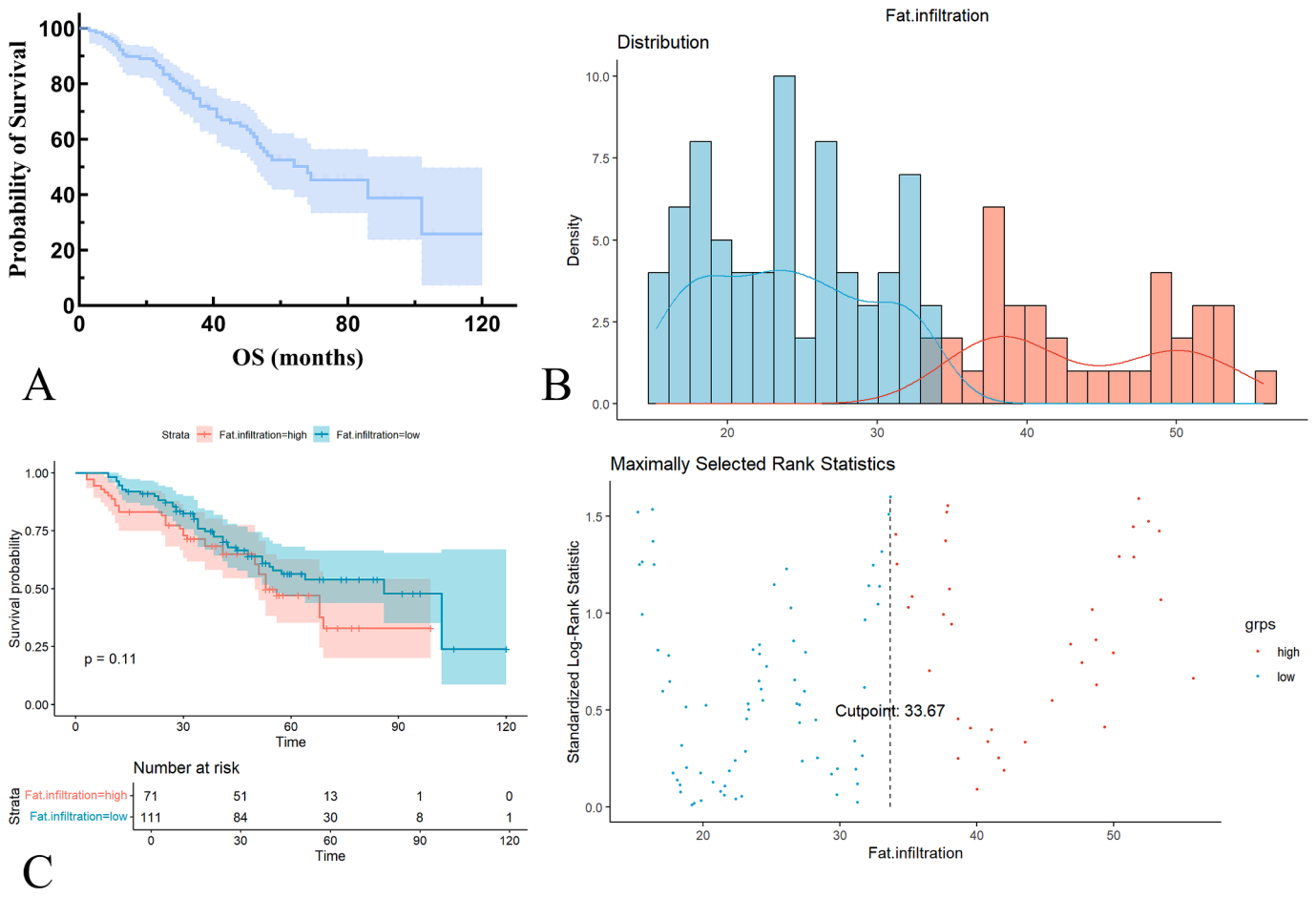

Fig. 2. Survival curves (A) Kaplan-Meier survival curve for 182 patients. (B) Distribution of patients across different fat infiltration rate intervals, with a cut-off value of 33.67 % based on survival data. (C) Log-rank test for groups divided by the cut-off value of 33.67 %.

Table 2
Univariate regression analysis results.

Parameters	Univariate logistic regression			Univariate linear regression		
	OR	95 %CI	P value	Coefficient	95 %CI	P value
Age	1.015	(0.985, 1.045)	0.328	0.504	(0.236, 0.772)	0.000*
Sex	0.846	(0.471, 1.519)	0.575	−12.534	(−17.767, −7.301)	0.000*
ISS stage	1.468	(0.939, 2.294)	0.093*	3.298	(−0.831, 7.427)	0.117
RBC	0.942	(0.674, 1.316)	0.725	−5.437	(−8.505, −2.369)	0.001*
Hb	0.998	(0.986, 1.009)	0.665	−0.183	(−0.286, −0.080)	0.001*
HCT	0.986	(0.948, 1.025)	0.479	−0.592	(−0.950, −0.234)	0.001*
Serum phosphorus	2.612	(0.936, 7.285)	0.067*	2.548	(−6.671, 11.767)	0.586
Fat infiltration rate	1.054	(1.031, 1.077)	0.000*	——	——	——

*, $P < 0.1$.
ISS, International Staging System; RBC, Red Blood Cell count; Hb, Hemoglobin; HCT, Hematocrit.

FIR as the independent variable, univariate COX regression analysis was performed, yielding P = 0.852, HR = 0.999, 95 % CI (0.985, 1.013), cut-off = 33.67 %, and statistic = 1.600 (Fig. 2***B***). Using 33.67 % as the grouping criterion, the log-rank test also showed no statistical significance (P = 0.11, Fig. 2***C***).

Using fracture occurrence as the dependent variable and FIR as the independent variable, univariate logistic regression analysis was performed, yielding P = 0.000, OR = 1.054, 95 % CI (1.031–1.077). The higher the patient's FIR, the greater the risk of fracture. Further univariate logistic regression analysis of other variables identified ISS stage and serum phosphorus as potential factors influencing fractures (P < 0.1, Table 2).

FIR, ISS stage, serum phosphorus, and LDH (variables with significant differences between groups, P < 0.05) were included in multivariate logistic regression, and FIR was identified as an independent factor influencing lumbar fractures (P < 0.05). The − 2 Log Likelihood was 218.765, Cox & Snell R^2 was 0.156, Nagelkerke R^2 was 0.209, and the Hosmer-Lemeshow statistic was 3.126 with a p-value of 0.926, indicating a good fit of the regression. The AUC was 0.715 (Fig. 3***A***), 95 % CI (0.639–0.790), P = 0.000, indicating a high predictive ability of the model, with a cut-off value of 31.81 %.

3.3. *Exploratory subgroup analysis*

Using FIR as the dependent variable, univariate linear regression analysis identified age, sex, RBC, Hb, and HCT as potential influencing

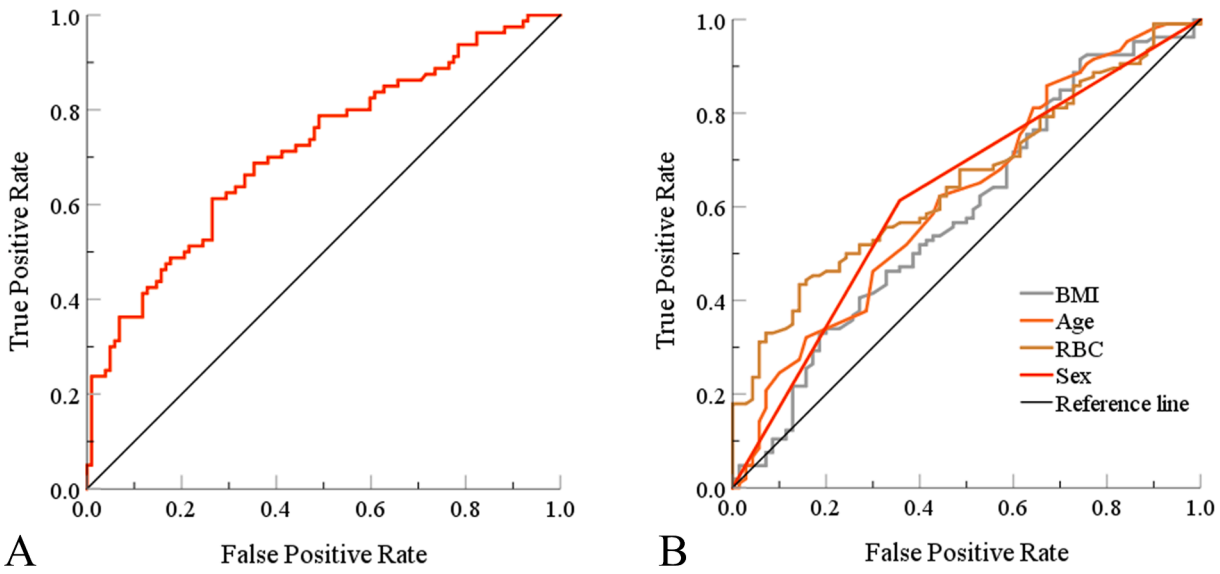

Fig. 3. Receiver Operating Characteristic curve (A) Using fracture as the state variable, independent factors influencing fractures identified through multivariate logistic regression were used as test variables to draw the Receiver Operating Characteristic curve. (B) Using FIR grouping (cut-off = 31.81 %) as the state variable, independent factors influencing FIR identified through multivariate linear regression were used as test variables to draw the Receiver Operating Characteristic curve. BMI, Body Mass Index; RBC, Red Blood Cell. (For interpretation of the references to colour in this figure legend, the reader is referred to the web version of this article.)

Table 3
Independent predictors affecting fat infiltration rate.

Parameter	Linear regression			ROC			
	Coefficient	95 %CI	P	AUC	95 %CI	P	Cut-off
Age	0.482	(0.233, 0.732)	< 0.001*	0.620	(0.535, 0.704)	0.007*	67.50
Sex	−11.771	(−16.583, −6.960)	< 0.001*	0.628	(0.544, 0.712)	0.004*	——
RBC	−3.946	(−6.782, −1.111)	0.007*	0.654	(0.574, 0.733)	0.001*	3.68
BMI	1.040	(0.293, 1.788)	0.007*	0.585	(0.498, 0.672)	0.057	27.40

*, P < 0.05.
ROC, Receiver Operating Characteristic; AUC, Area Under the ROC Curve; RBC, Red Blood Cell count; BMI, Body Mass Index.

factors (P < 0.1, Table 2). Multivariate linear regression analysis identified age, sex, RBC, and BMI as independent factors influencing FIR (P < 0.05, Table 3). Groups based on FIR cut-off values derived from fracture status were used as the state variable, while the independent influencing factors of FIR were used as the test variables. ROC curves were plotted (Fig. 3***B***), and the AUC and corresponding cut-off values were subsequently calculated (Table 3).

To avoid small sample sizes in subgroups, patients were grouped by sex, median age [57 years (52.0, 66.25)], WHO BMI classification (BMI < 25 kg/m^2 for underweight/normal, BMI ≥ 25 kg/m^2 for overweight), and RBC count based on cut-off (3.68 × 10^12/L). A forest plot was created (Fig. 4). In the overall population, FIR's predictive ability for fractures did not show significant interaction with age, sex, RBC count, or BMI, with P for interaction > 0.05. Among patients with BMI ≥ 25 kg/m2, P = 0.120, and among patients with RBC > 3.68 × 10^12/L, P = 0.117, the association between FIR and fractures was weakened in these subgroups.

3.4. Development and validation of the nomogram for fat infiltration rate

A nomogram was developed based on the multivariate linear regression results for FIR (Fig. 5***A***). Each predictive factor is assigned a scoring line. The total score is calculated by adding the scores of each variable. By drawing a vertical line from the total score to the value on the bottom x-axis, the probability of a paraspinal muscle FIR > 31.81 %. The model's C-index was 0.777, 95 % CI (0.707–0.846), indicating good discrimination (Fig. 5***B***). In the calibration curve, the x-axis represents the predicted probability of adverse outcomes by the nomogram, while the y-axis represents the actual probability of adverse outcomes. The ideal curve corresponds to a 45°diagonal line, representing a perfect predictive model. The apparent curve represents the actual data of the entire cohort (N = 182), and the bias-corrected curve is obtained through bootstrapping (B = 1000 repetitions) to correct any bias. The calibration curve showed that the ideal and apparent lines were very close, with a mean absolute error of 0.011, a mean squared error of 0.00024, and a quantile of absolute error = 0.029, indicating high model consistency (Fig. 5***C***). In the DCA, the y-axis represents standardized net benefit, and the x-axis represents the high-risk threshold. The horizontal line represents "none," indicating no intervention for all patients, resulting in a net benefit of 0. The diagonal line represents "all," indicating intervention for all patients, with a negative net benefit curve slope. The curve above the "none" and "all" lines indicated net benefit >0, demonstrating good clinical guidance benefits of the model within this range (Fig. 5***D***). The small difference between the prediction curve and the actual disease curve in the CIC suggests that the model aligns well with actual situation (Fig. 5***E***).

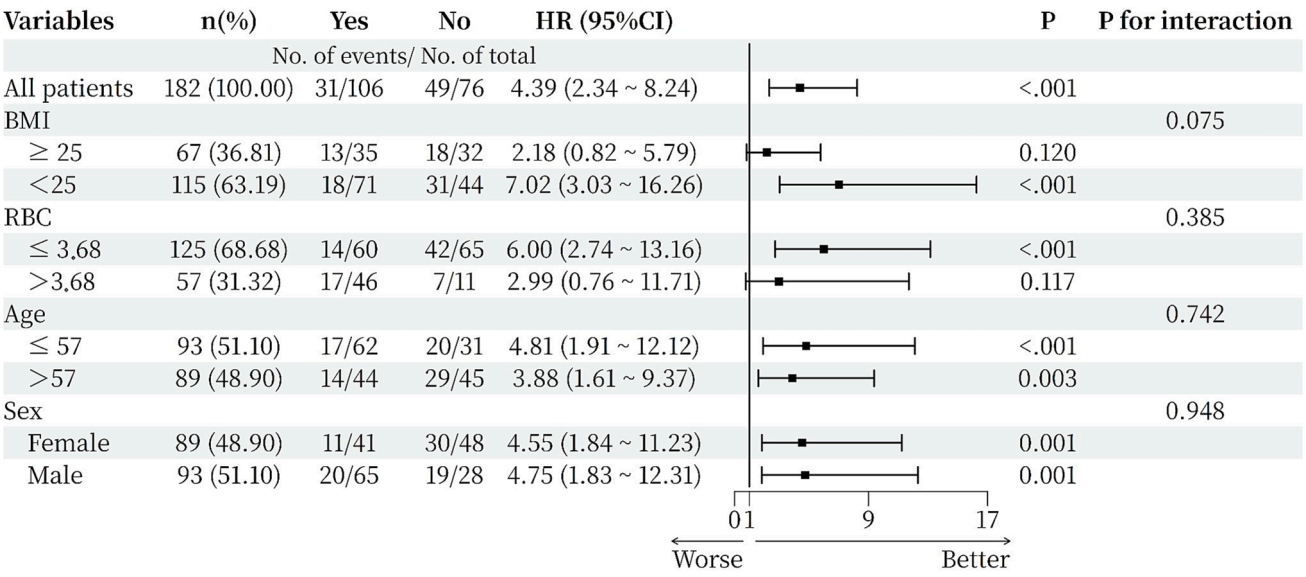

Fig. 4. The forest plot of the subgroup analysis on the relationship between fat infiltration rate (FIR) and fractures. The mean FIR for patients with BMI < 25 kg/m^2 was 31.74 ± 17.62 %, while for those with BMI ≥ 25 kg/m^2, it was 35.98 ± 20.81 %. The mean FIR for patients with RBC count ≤ 3.68 × 10^12/L was 36.51 ± 20.49 %, while for those with RBC count > 3.68 × 10^12/L, it was 26.28 ± 12.38 %. The mean FIR for patients aged ≤ 57 years was 29.35 ± 16.06 %, while for those aged > 57 years, it was 37.44 ± 20.79 %. The mean FIR for female patients was 39.71 ± 20.81 %, while for male patients, it was 27.18 ± 14.55 %.

4. Discussion

Myosteatosis, characterized by abnormal adipose tissue distribution within and between muscle cells, results in excessive fat deposition within the muscle, which is a pathological state linked to diminished muscle mass, limb functionality and physical performance [17], which increases the risk of adverse outcomes in patients [6]. Referring to previous research methods [12,13,15,16], we measured the FIR of the erector spinae and multifidus muscles at the L3 level in 182 patients at our center. The average FIR in patients with MM was 33.30 %, significantly higher than in the healthy population (12–15 %) [18]. This may be related to the imbalance in muscle proliferation and differentiation caused by the high expression of sclerostin in muscle tissue of MM patients [19]. Moreover, the m6A-RCD axis is an important pathway in MM progression, affecting MM's invasiveness to musculoskeletal tissues and contributing to the occurrence of myosteatosis [20].

Several studies have indicated that sarcopenia in hematological diseases like lymphoma and aplastic anemia is associated with shorter survival times. In the context of MM, Williams et al. [7] found that 51 % of MM patients had muscle loss, which was associated with early cardiovascular complications following stem cell transplantation. However, our study did not find a significant association between FIR and patient survival outcomes. Although survival curves suggest that the low-FIR group might have a longer survival trend, the log-rank test showed no statistical significance, possibly due to the small number of patients included. On the other hand, comprehensive muscle loss mainly increases mortality risk by affecting respiratory function [21]. MM patients often suffer from multi-organ damage, and fatal complications in other systems, such as infection or renal failure, may occur earlier than the lethal point of paraspinal muscle degeneration, possibly masking the impact of myosteatosis on MM patient survival.

As previously mentioned, in the context of significantly extended survival rates for MM, the prognosis of MM needs to be considered from two aspects. In addition to survival outcomes, it is equally important to analyze the impact of myosteatosis on patients' quality of life.

In clinical work, we have observed that some patients who respond well to chemotherapy still experience significant low back pain after the treatment cycle, which is puzzling. Myosteatosis seems to be a reasonable explanation for the persistent low back pain in these patients. In this study, patients with higher FIR had more severe low back pain, consistent with the findings of Suzuki K et al. [22]. The mechanism by which myosteatosis causes low back pain can be explained in several ways. First, adipose tissue is one of the major sources of pro-inflammatory cytokines, and local inflammatory activity caused by fat infiltration in paraspinal muscles exacerbates low back muscle pain [23]. Additionally, biomechanical data indicate that 40 % to 49 % of the total force needed to maintain lumbar posterior rotation and stability is contributed by low-segment muscle fibers [24]. When fat infiltrates the multifidus and erector spinae muscles at low segments, core muscle strength declines, leading to dynamic imbalance in the lumbar facet joints and adjacent soft tissues, resulting in damage or spasms of the surrounding muscles, causing foraminal edema, and stimulating nerve endings, which manifests as muscle soreness and pain [25]. Functionally, when vertebral displacement exceeds the neutral zone, paraspinal muscles infiltrated with fat may struggle to coordinate and maintain vertebral stability [26]. Patients may exert more effort to maintain balance, resulting in poorer performance in daily activities. In this study, patients with higher FIR had significantly higher ODI (23.19 ± 11.00 %) vs (16.91 ± 9.31 %) compared to the low-FIR group, indicating that myosteatosis could be a potential predictor of functional impairment in MM patients [27].

Myosteatosis alters the mechanical structure of the spine and disrupts its original balance, significantly increasing the stress borne by the vertebral body [28]. Moreover, molecular signaling pathways linking muscle and bone exist in the body, and muscle loss is often accompanied by osteoporosis [29]. These factors, combined with the osteolytic characteristics of MM, greatly increase the risk of fractures in MM patients. However, spinal fracture symptoms in MM patients are usually mild, and some mild to moderate spinal fractures are difficult to notice. Previous studies by Ikchan et al. have confirmed that paraspinal fat degeneration can be a predictor of vertebral collapse progression [30]. Therefore, analyzing the relationship between myosteatosis and fractures in MM patients is of great clinical significance. Our study found that the risk of fractures increased significantly with elevated FIR. We further conducted subgroup analysis to exclude confounding factors. When BMI ≥ 25 kg/m^2 or RBC count >3.68 × 10^12/L, the predictive power of FIR for fractures was weakened. With a higher BMI, patients may experience widespread heterogeneity in systemic fat distribution, causing local measurements to fail in fully reflecting the overall risk [31]. Furthermore, metabolic disturbances induced by elevated BMI

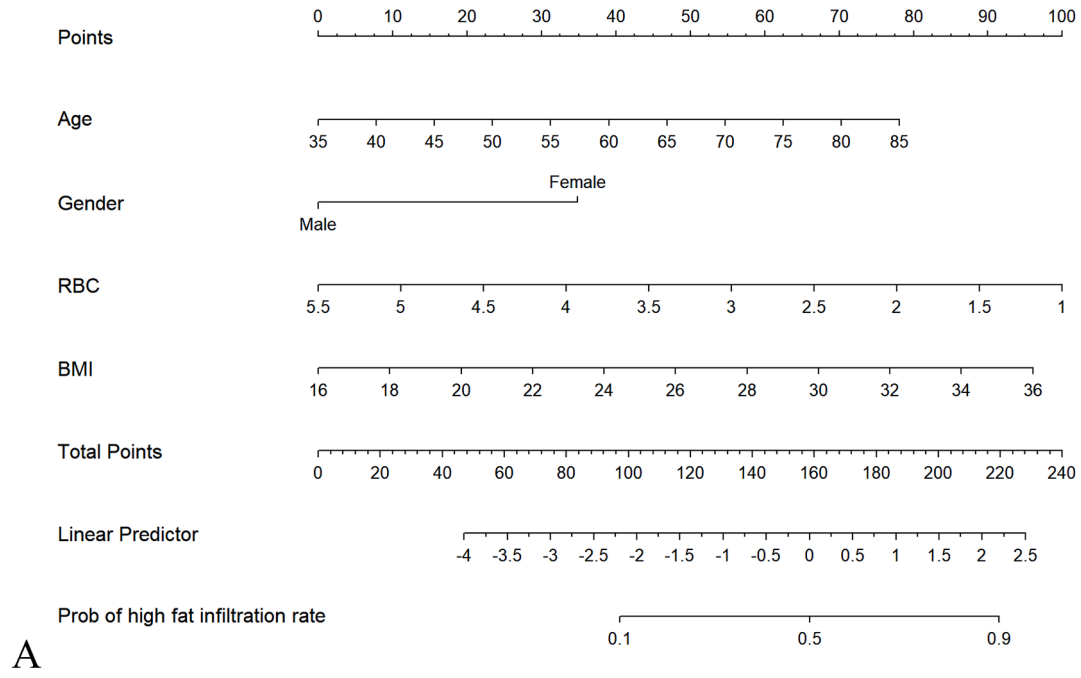

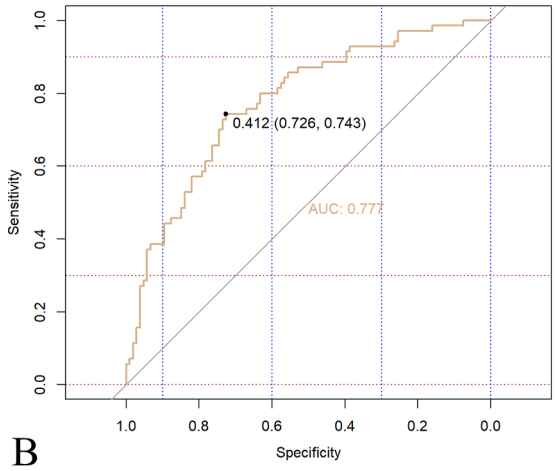

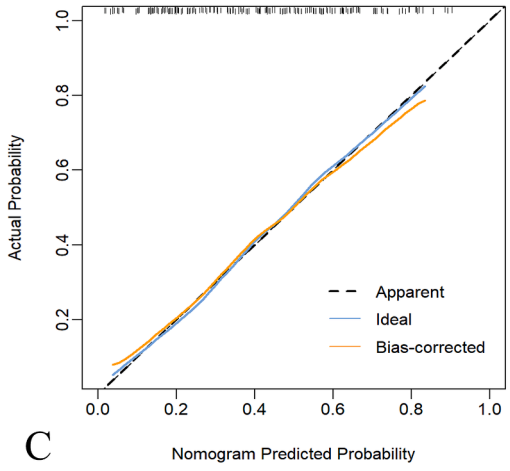

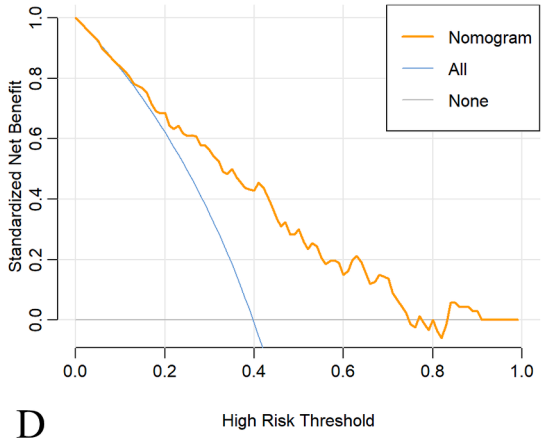

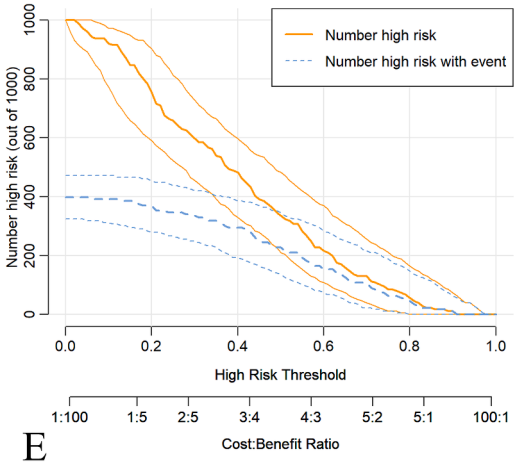

Fig. 5. The nomogram and validation plot for the fat infiltration rate in patients with multiple myeloma (A) Nomogram: RBC, Red Blood Cell count; BMI, Body Mass Index. (B) Receiver operating characteristic curve for the FIR predictive model. (C) Calibration curve of the nomogram. (D) Decision curve analysis of the nomogram. (E) Clinical impact curve of the nomogram: In a population size of 1000, under different thresholds, the orange line represents those identified as high risk by the model, and the blue line below represents the actual number of outcome events among the high-risk population. (For interpretation of the references to colour in this figure legend, the reader is referred to the web version of this article.)

levels – including insulin resistance and hyperlipidemia [32] – combined with chronic low-grade inflammation [33] and adverse clinical outcomes [34], collectively disrupt bone metabolic homeostasis. These multifaceted pathophysiological mechanisms may substantially attenuate the direct impact of adipose tissue infiltration on fracture risk. A normal red blood cell count may indicate that the hematopoietic microenvironment has not been severely damaged, and that the patient has relatively high levels of antioxidant enzymes, which to some extent counteract the progression of bone damage [35]. However, in the general population, FIR still maintains specificity in predicting fractures. This phenomenon suggests that patients with limited mobility should be encouraged to engage in functional exercises. During surgery, attention should be paid to protecting the paraspinal muscles to avoid iatrogenic muscle denervation, which could lead to muscle atrophy [36].

Our study identified significant correlations between age, sex, BMI, and RBC levels with patients' FIR. The nomogram model incorporating these four parameters demonstrated favorable predictive performance with significant clinical utility, achieving a C-index of 0.777. Currently, there is a paucity of research investigating determinants of MM-associated myosteatosis. Studies in other disease domains have revealed distinct predictive markers: the creatinine-to-cystatin C ratio emerged as an independent predictor for myosteatosis in gastrointestinal cancer patients [37];γ-glutamyltransferase showed strong associations with myosteatosis in healthy populations [37], while low serum manganese concentrations were significantly linked to myosteatosis in cirrhotic patients [38]. Notably, the reported C-indices for these biomarkers across studies ranged from 0.59 to 0.85. Comparative analysis of C-index values reveals that while our prediction model exhibits moderate discriminative ability within this spectrum, its performance remains inferior to certain sophisticated models. Future refinements through multi-omics integration or inclusion of additional sensitive predictors may substantially enhance the model's predictive accuracy.

Inflammation during aging leads to the redistribution of fat to intra-abdominal regions and skeletal muscles. Lipids and their derivatives accumulate within and between muscle cells, inducing mitochondrial dysfunction, disrupting fatty acid β-oxidation, increasing reactive oxygen species, and enhancing the secretion of pro-inflammatory cytokines. These factors, in turn, exacerbate chronic inflammation, establish local hyperlipidemia, and form a vicious cycle of fat redistribution, insulin resistance, and inflammation, promoting muscle fat infiltration [39]. Studies have shown that the FIR of the multifidus muscle (>0.18 %/year), erector spinae muscle (>0.13 %/year), and psoas muscle (>0.04 %/year) in elderly Asians slowly increases with age. The degree of fat infiltration in our patient cohort was also related to age. Patients below the median age (≤57 years) had an average FIR of 29.35 %, while those above the median age (>57 years) had an average FIR of 37.44 %. Additionally, age-related changes in skeletal muscle mass are influenced by gender differences. Crawford et al. [18] studied 80 healthy individuals and found that the FIR in females was about 15 %, while in males, it was about 12 %. Using the same measurement method, we observed that the average FIR in female MM patients was 39.71 %, compared to 27.18 % in male patients, indicating a higher degree of fat infiltration in females. This phenomenon was also reflected in muscle volume changes, with a significantly higher prevalence of sarcopenia in females than in males (71.26 % vs. 32.6 %) [19]. Hormonal dysfunction may explain the more pronounced muscle loss in females. Testosterone can activate protein synthesis and inhibit the activity of pre-adipocyte progenitor cells [40]. While testosterone levels in men decrease by about 1 % annually after age 30, in women, testosterone levels decline rapidly between the ages of 20 and 45 [41]. The differences in testosterone levels make female patients more prone to myosteatosis. Sarcopenia and obesity are both multifactorial syndromes with various overlapping and feedback mechanisms. In obese patients, cytokine paracrine signaling can cause muscle progenitor cells to differentiate into an adipocyte-like phenotype, leading to muscle loss and increased fat infiltration [42]. Myosteatosis, often accompanied by skeletal muscle atrophy and persistent secretion of pro-inflammatory cytokines, represents a unique state of fat redistribution that increases the risk of obesity in adults [43]. Our study found a positive correlation between FIR levels and BMI, consistent with the findings of Vivodtzev I et al. [43] in patients with COPD. Additionally, patients with high FIR had significantly lower levels of red blood cells, hemoglobin, and hematocrit. This phenomenon has also been observed in diabetic patients [44]. As the abovementioned, increased oxidative stress in skeletal muscle is a key factor leading to muscle loss. The oxidative status of red blood cells (presence of antioxidant enzymes) enables them to neutralize free radicals and reduce oxidative damage [35]. Therefore, a decrease in the number of red blood cells weakens the body's ability to counteract oxidative stress, increasing the risk of myosteatosis.

MM patients require long-term pharmacological support, and studies have identified potential associations between certain chemotherapeutic agents and myosteatosis [45]. Bortezomib, a targeted therapy for MM, disrupts multiple signaling pathways in MM cells, arrests the cell cycle, and induces apoptosis and cell death [46]. However, it may concurrently promote muscle catabolism via pathways such as PI3K/Akt/mTOR [47]. Guglielmi et al. [48] demonstrated that exposure of MM patient-derived skeletal muscle myoblasts to high concentrations of bortezomib for 72 h reduced primary myotube survival, potentially linked to lipid droplet accumulation and mitochondrial structural/functional impairments in myoblasts. Notably, our prior study found no significant association between bortezomib-based chemotherapy and sarcopenia risk [49], which may reflect confounding effects from concurrent medications or limited sample size. The mechanisms underlying bortezomib's impact on myosteatosis in MM patients remain to be elucidated. Endocrine alterations—including reduced androgen and growth factor levels, alongside glucocorticoid use—also critically influence myosteatosis progression [50]. Glucocorticoids have been shown to directly suppress muscle stem cell function via myostatin upregulation, contributing to muscle atrophy [51], while stimulating skeletal muscle protein breakdown and inhibiting synthesis, particularly in type II fibers responsible for dynamic function [52]. These pharmacological targets warrant further exploration to inform novel interventions for myosteatosis. For instance, 11β-HSD1 inhibition mitigates glucocorticoid-induced protein degradation in murine myotubes and human primary myoblasts [53,54], highlighting its therapeutic potential. Androgen receptor modulators, such as selective androgen receptor modulators, exhibit dual anabolic and anti-catabolic effects on differentiated myotubes, preserving muscle mass in sarcopenia patients and selectively promoting muscle growth [55]. Complementing these targeted therapies, multimodal management strategies are essential—tailored exercise regimens (aerobic/resistance training) [56] and optimized nutrition synergistically counteract metabolic dysregulation, whereas extracorporeal shock wave therapy enhances functional recovery through improved perfusion, spasm relief, and endogenous repair activation [57].

Our study has several strengths. First, it explores and analyzes the impact of myeloma-related myosteatosis on patient prognosis from a novel orthopedic perspective, integrating deeply with clinical practice. Second, the significant findings of this study were visualized and validated, using rigorous statistical methods to reduce bias, providing high clinical relevance. However, certain limitations must be acknowledged. The single-center design restricts generalizability across diverse ethnic populations. Although fat infiltration was more pronounced in the erector spinae and multifidus muscles compared to other muscle groups, independent analyses of myosteatosis in other musculature remain warranted. During the follow-up period, treatment modifications in some patients, combined with the limited sample size, precluded the analysis of certain variables of interest, such as the relationship between treatment regimens and myosteatosis. In future studies, we plan to conduct multi-center prospective research to comprehensively investigate the association between myosteatosis and clinical outcomes in MM patients, alongside in-depth etiological analyses.

5. Conclusions

This study describes and analyzes the clinical value of myosteatosis in MM patients from a novel perspective. It also examines the factors influencing the FIR in MM patients. Some important clinical conclusions were drawn: Myosteatosis characterized by FIR is not a reliable indicator of survival prognosis in MM patients, but it can be used as a predictor of fractures and is closely related to low back pain and functional impairment. FIR is significantly correlated with age, gender, RBC, and BMI. When BMI $\geq$ 25 kg/m^2 or RBC count >3.68 $\times$ 10^12/L, the predictive power of FIR for fractures decreases.

Author contributions

JPL, XCY, and XJS contributed to conception and design of the study. ZYX and MS contributed to the data collection. JPL contributed to the data analysis and wrote the first draft of the manuscript. JPL and ML designed the figures and tables. XRD and YW critically revised the manuscript. All authors have read and approved the submitted version.

CRediT authorship contribution statement

Jun-Peng Liu: Writing – original draft, Visualization, Formal analysis, Conceptualization. **Xing-Chen Yao:** Conceptualization. **Ming Shi:** Data curation. **Zi-Yu Xu:** Data curation. **Yue Wu:** Writing – review & editing. **Xiang-Jun Shi:** Conceptualization. **Meng Li:** Visualization. **Xin-Ru Du:** Writing – review & editing.

Declaration of competing interest

The authors declare that they have no known competing financial interests or personal relationships that could have appeared to influence the work reported in this paper.

Data Availability

The datasets used and/or analyzed during the current study are available from the corresponding author on reasonable request.

References

[1] A. Koschmieder, O. Stachs, B. Kragl, T. Stahnke, K.A. Sterenczak, L. Henze, A. G. Jünemann, C. Junghanss, R.F. Guthoff, H. Murua Escobar, Non-invasive detection of corneal sub-basal nerve plexus changes in multiple myeloma patients by confocal laser scanning microscopy, Biosci. Rep. 40 (10) (2020).

[2] M.A. Papadimitriou, K. Soureas, A.M. Papanota, P. Tsiakanikas, P.G. Adamopoulos, I. Ntanasis-Stathopoulos, P. Malandrakis, M. Gavriatopoulou, D.C. Sideris, E. Kastritis, M. Avgeris, M.A. Dimopoulos, E. Terpos, A. Scorilas, miRNA-seq identification and clinical validation of CD138+ and circulating miR-25 in treatment response of multiple myeloma, J. Transl. Med. 21 (1) (2023) 245.

[3] M. Baghdadi, K. Ishikawa, S. Nakanishi, T. Murata, Y. Umeyama, T. Kobayashi, Y. Kameda, H. Endo, H. Wada, B. Bogen, S. Yamamoto, K. Yamaguchi, I. Kasahara, H. Iwasaki, M. Takahata, M. Ibata, S. Takahashi, H. Goto, T. Teshima, K.I. Seino, A role for IL-34 in osteolytic disease of multiple myeloma, Blood Adv. 3 (4) (2019) 541–551.

[4] G. Chawla, N. Dutt, K. Deokar, V.K. Meena, Chest pain without a clue-ultrasound to rescue occult multiple myeloma: A case report, World J. Radiol. 11 (12) (2019) 144–148.

[5] M. Nachit, M. De Rudder, J.P. Thissen, O. Schakman, C. Bouzin, Y. Horsmans, G. Vande Velde, I.A. Leclercq, Myosteatosis rather than sarcopenia associates with non-alcoholic steatohepatitis in non-alcoholic fatty liver disease preclinical models, J. Cachexia. Sarcopenia Muscle 12 (1) (2021) 144–158.

[6] G. Han, Y. Jiang, B. Zhang, C. Gong, W. Li, Imaging Evaluation of Fat Infiltration in Paraspinal Muscles on MRI: A Systematic Review with a Focus on Methodology, Orthop. Surg. 13 (4) (2021) 1141–1148.

[7] A. Williams, D. Baruah, J. Patel, A. Szabo, S. Chhabra, B. Dhakal, P. Hari, S. Janz, M. Stolley, A. D'Souza, Prevalence and significance of sarcopenia in multiple myeloma patients undergoing autologous hematopoietic cell transplantation, Bone Marrow Transplant. 56 (1) (2021) 225–231.

[8] T.D. Diallo, A.I.L. Blessing, G. Ihorst, M.D. Möller, P.M. Jungmann, F. Bamberg, G. Herget, R. Wäsch, M. Engelhardt, J. Neubauer, Myosteatosis in multiple myeloma: a key determinant of survival beyond sarcopenia, Skeletal Radiol. 54 (2) (2025) 275–285.

[9] N.H. Abdallah, H. Nagayama, N. Takahashi, W. Gonsalves, A. Fonder, A. Dispenzieri, D. Dingli, F.K. Buadi, M.Q. Lacy, M. Hobbs, M.A. Gertz, M. Binder, P. Kapoor, R. Warsame, S.R. Hayman, T. Kourelis, Y.L. Hwa, Y. Lin, R.A. Kyle, S. V. Rajkumar, S.M. Broski, S.K. Kumar, Muscle and fat composition in patients with newly diagnosed multiple myeloma, Blood Cancer J. 13 (1) (2023) 185.

[10] J. Guan, D. Zhao, T. Liu, X. Yu, N. Feng, G. Jiang, W. Li, K. Yang, H. Zhao, Y. Yang, Correlation between surgical segment mobility and paravertebral muscle fatty infiltration of upper adjacent segment in single-segment LDD patients: retrospective study at a minimum 2 years' follow-up, BMC Musculoskelet. Disord. 24 (1) (2023) 28.

[11] J. Chen, Y. Huang, X. Zeng, J. Ma, X. Huang, H. Liang, B. He, Functional magnetic resonance imaging reveals dysfunction of the paraspinal muscles in patients with chronic low back pain: a cross-sectional study, Quant. Imaging Med. Surg. 13 (6) (2023) 3416–3427.

[12] K. Takayama, T. Kita, H. Nakamura, F. Kanematsu, T. Yasunami, H. Sakanaka, Y. Yamano, New predictive index for lumbar paraspinal muscle degeneration associated with aging, Spine 41 (2) (2016) E84–E90.

[13] M. Fortin, M.C. Battié, Quantitative paraspinal muscle measurements: inter-software reliability and agreement using OsiriX and ImageJ, Phys. Ther. 92 (6) (2012) 853–864.

[14] A. Saifuddin, R. Rajakulasingam, R. Santiago, M. Siddiqui, M. Khoo, I. Pressney, Comparison of lumbar degenerative disc disease using conventional fast spin echo T(2)W MRI and T(2) fast spin echo dixon sequences, Br. J. Radiol. 94 (1121) (2021) 20201438.

[15] A.J. Cruz-Jentoft, G. Bahat, J. Bauer, Y. Boirie, O. Bruyère, T. Cederholm, C. Cooper, F. Landi, Y. Rolland, A.A. Sayer, S.M. Schneider, C.C. Sieber, E. Topinkova, M. Vandewoude, M. Visser, M. Zamboni, Sarcopenia: revised European consensus on definition and diagnosis, Age Ageing 48 (4) (2019) 601.

[16] R.J. Crawford, J. Cornwall, R. Abbott, J.M. Elliott, Manually defining regions of interest when quantifying paravertebral muscles fatty infiltration from axial magnetic resonance imaging: a proposed method for the lumbar spine with anatomical cross-reference, BMC Musculoskelet. Disord. 18 (1) (2017) 25.

[17] Z. Du, Y. Xiao, G. Deng, H. Song, Y. Xue, H. Song, CD3+/CD4+ cells combined with myosteatosis predict the prognosis in patients who underwent gastric cancer surgery, J. Cachexia. Sarcopenia Muscle 15 (4) (2024) 1587–1600.

[18] R.J. Crawford, L. Filli, J.M. Elliott, D. Nanz, M.A. Fischer, M. Marcon, E.J. Ulbrich, Age- and level-dependence of fatty infiltration in lumbar paravertebral muscles of healthy volunteers, AJNR Am. J. Neuroradiol. 37 (4) (2016) 742–748.

[19] J. Ren, J. Wang, X. Yao, Y. Wu, M. Shi, X. Shi, X. Du, Investigation of the underlying mechanism of sclerosteosis expression in muscle tissue in multiple myeloma with sarcopenia, J. Inflamm. Res. 16 (2023) 563–578.

[20] J. Han, C. Wang, H. Yang, J. Luo, X. Zhang, X.A. Zhang, Novel insights into the links between N6-methyladenosine and regulated cell death in musculoskeletal diseases, Biomolecules 14 (5) (2024).

[21] R. Kob, C. Fellner, T. Bertsch, A. Wittmann, D. Mishura, C.C. Sieber, B.E. Fischer, C. Stroszczynski, C.L. Bollheimer, Gender-specific differences in the development of sarcopenia in the rodent model of the ageing high-fat rat, J. Cachexia. Sarcopenia Muscle 6 (2) (2015) 181–191.

[22] K. Suzuki, Y. Hasebe, M. Yamamoto, K. Saita, S. Ogihara, Risk factor analysis for fat infiltration in the lumbar paraspinal muscles in patients with lumbar degenerative diseases, Geriatr. Orthop. Surg. Rehabil. 13 (2022) 21514593211070688.

[23] X. Chen, W. Wang, P. Cui, Y. Li, S. Lu, Evidence of MRI image features and inflammatory biomarkers association with low back pain in patients with lumbar disc herniation, Spine J. 24 (7) (2024) 1192–1201.

[24] C.P. Gabel, H.R. Mokhtarinia, M. Melloh, The politics of chronic LBP: can we rely on a proxy-vote? linking multifidus intra-myo-cellular lipid (IMCL) fatty infiltration with arthrogenic muscle inhibition (AMI)-induced chronic nonspecific low back pain, Spine (Phila Pa 1976) 46 (2) (2021) 129–130.

[25] G.A. Matarán-Peñarrocha, I.C. Lara Palomo, E. Antequera Soler, E. Gil-Martínez, M. Fernández-Sánchez, M.E. Aguilar-Ferrándiz, A.M. Castro-Sánchez, Comparison of efficacy of a supervised versus non-supervised physical therapy exercise program on the pain, functionality and quality of life of patients with non-specific chronic low-back pain: a randomized controlled trial, Clin. Rehabil. 34 (7) (2020) 948–959.

[26] Y. Liu, Y. Liu, Y. Hai, T. Liu, L. Guan, X. Chen, Y. Wang, Multifidus muscle fatty infiltration as an index of dysfunction in patients with single-segment degenerative lumbar spinal stenosis: a case-control study based on propensity score matching, J. Clin. Neurosci. 75 (2020) 139–148.

[27] M. Fortin, À. Lazáry, P.P. Varga, M.C. Battié, Association between paraspinal muscle morphology, clinical symptoms and functional status in patients with lumbar spinal stenosis, Eur. Spine J. 26 (10) (2017) 2543–2551.

[28] S.Q. Chen, Q.P. Li, Y.Y. Huang, A.N. Guo, R.F. Zhang, P.P. Ye, Z.H. Yan, J.W. He, Different spinal subtypes with varying characteristics of lumbar disc degeneration at specific level with age: a study based on an asymptomatic population, J. Orthop. Surg. Res. 15 (1) (2020) 3.

[29] H. Kaji, Effects of myokines on bone, Bonekey Rep. 5 (2016) 826.

[30] I. Jeon, S.W. Kim, D. Yu, Paraspinal muscle fatty degeneration as a predictor of progressive vertebral collapse in osteoporotic vertebral compression fractures, Spine J. 22 (2) (2022) 313–320.

[31] F. Petrelli, A. Cortellini, A. Indini, G. Tomasello, M. Ghidini, O. Nigro, M. Salati, L. Dottorini, A. Iaculli, A. Varricchio, V. Rampulla, S. Barni, M. Cabiddu, A. Bossi, A. Ghidini, A. Zaniboni, Association of obesity with survival outcomes in patients with cancer: a systematic review and meta-analysis, JAMA Netw. Open 4 (3) (2021) e213520.

[32] G.R.F. Collaborators, Global, regional, and national comparative risk assessment of 84 behavioural, environmental and occupational, and metabolic risks or clusters of

risks for 195 countries and territories, 1990-2017: a systematic analysis for the Global Burden of Disease Study 2017, Lancet (London, England) 392 (10159) (2018) 1923–1994.
[33] H.S. Park, J.Y. Park, R. Yu, Relationship of obesity and visceral adiposity with serum concentrations of CRP, TNF-alpha and IL-6, Diabetes Res. Clin. Pract. 69 (1) (2005) 29–35.
[34] E.M. Bullwinkle, M.D. Parker, N.F. Bonan, L.G. Falkenberg, S.P. Davison, K. L. DeCicco-Skinner, Adipocytes contribute to the growth and progression of multiple myeloma: unraveling obesity related differences in adipocyte signaling, Cancer Lett. 380 (1) (2016) 114–121.
[35] I. Ghzaiel, A. Zarrouk, V. Pires, J.P. de Barros, S. Hammami, M. Ksila, M. Hammami, T. Ghrairi, P. Jouanny, A. Vejux, G. Lizard, 7β-Hydroxycholesterol and 7-ketocholesterol: new oxidative stress biomarkers of sarcopenia inducing cytotoxic effects on myoblasts and myotubes, J. Steroid Biochem. Mol. Biol. 232 (2023) 106345.
[36] S. Hoppe, D. Maurer, W. Valenzuela, L.M. Benneker, S.F. Bigdon, S. Häckel, S. Wangler, C.E. Albers, 3D analysis of fatty infiltration of the paravertebral lumbar muscles using T2 images-a new approach, Eur. Spine J. 30 (9) (2021) 2570–2576.
[37] H. Liu, J. Wang, S. Tan, Z. Zhang, M. Yan, J. Han, X. Sui, F. Yang, G. Wu, Sarcopenia and myosteatosis diagnostic tool for gastrointestinal cancer: creatinine to cystatin C ratio as evaluation marker, J. Transl. Med. 21 (1) (2023) 744.
[38] X. Zhang, W. Yang, G. Guo, W. Liu, C. Sun, Low serum manganese as a noninvasive marker predicting the presence of myosteatosis among hospitalized patients with cirrhosis, Nutr. Res. 126 (2024) 151–158.
[39] C.W. Li, K. Yu, N. Shyh-Chang, Z. Jiang, T. Liu, S. Ma, L. Luo, L. Guang, K. Liang, W. Ma, H. Miao, W. Cao, R. Liu, L.J. Jiang, S.L. Yu, C. Li, H.J. Liu, L.Y. Xu, R.J. Liu, X.Y. Zhang, G.S. Liu, Pathogenesis of sarcopenia and the relationship with fat mass: descriptive review, J. Cachexia. Sarcopenia Muscle 13 (2) (2022) 781–794.
[40] M.T. Haren, A.M. Siddiqui, H.J. Armbrecht, R.T. Kevorkian, M.J. Kim, M.J. Haas, A. Mazza, V.B. Kumar, M. Green, W.A. Banks, J.E. Morley, Testosterone modulates gene expression pathways regulating nutrient accumulation, glucose metabolism and protein turnover in mouse skeletal muscle, Int. J. Androl. 34 (1) (2011) 55–68.
[41] J.E. Morley, Sarcopenia in the elderly, Fam. Pract. 29 (Suppl 1) (2012) i44–i48.
[42] R. Kob, L.C. Bollheimer, T. Bertsch, C. Fellner, M. Djukic, C.C. Sieber, B.E. Fischer, Sarcopenic obesity: molecular clues to a better understanding of its pathogenesis? Biogerontology 16 (1) (2015) 15–29.
[43] I. Vivodtzev, L. Moncharmont, R. Tamisier, J.C. Borel, F. Arbib, B. Wuyam, P. Lévy, F. Maltais, G. Ferretti, J.L. Pépin, Quadriceps muscle fat infiltration is associated with cardiometabolic risk in COPD, Clin. Physiol. Funct. Imaging 38 (5) (2018) 788–797.
[44] H. Zhang, J. Wang, J. Xi, J. Xu, L. Wang, Functional fitness and risk factors of older patients with diabetes combined with sarcopenia and/or frailty: a cross-sectional study, Nurs. Open 11 (1) (2024) e2042.
[45] I.J. Rutten, D.P. van Dijk, R.F. Kruitwagen, R.G. Beets-Tan, S.W. Olde Damink, T. van Gorp, Loss of skeletal muscle during neoadjuvant chemotherapy is related to decreased survival in ovarian cancer patients, J. Cachexia. Sarcopenia Muscle 7 (4) (2016) 458–466.
[46] E. Kupperman, E.C. Lee, Y. Cao, B. Bannerman, M. Fitzgerald, A. Berger, J. Yu, Y. Yang, P. Hales, F. Bruzzese, J. Liu, J. Blank, K. Garcia, C. Tsu, L. Dick, P. Fleming, L. Yu, M. Manfredi, M. Rolfe, J. Bolen, Evaluation of the proteasome inhibitor MLN9708 in preclinical models of human cancer, Cancer Res. 70 (5) (2010) 1970–1980.
[47] S. Haberecht-Müller, E. Krüger, J. Fielitz, Out of control: the role of the ubiquitin proteasome system in skeletal muscle during inflammation, Biomolecules 11 (9) (2021).
[48] V. Guglielmi, D. Nowis, M. Tinelli, M. Malatesta, L. Paoli, M. Marini, P. Manganotti, R. Sadowski, G.M. Wilczynski, V. Meneghini, G. Tomelleri, G. Vattemi, Bortezomib-Induced Muscle Toxicity in Multiple Myeloma, J. Neuropathol. Exp. Neurol. 76 (7) (2017) 620–630.
[49] J. Ren, L. Qi, X.C. Yao, J.Z. Wang, X.J. Shi, W.M. Chen, X.R. Du, Analysis of risk factors for multiple myeloma combined with radiation-based sarcopenia, Chin. J. Orthopaedics 43 (9) (2023) 567–573.
[50] E. Gonzalez Rodriguez, P. Marques-Vidal, B. Aubry-Rozier, G. Papadakis, M. Preisig, C. Kuehner, P. Vollenweider, G. Waeber, D. Hans, O. Lamy, Diurnal salivary cortisol in sarcopenic postmenopausal women: the OsteoLaus Cohort, Calcif. Tissue Int. 109 (5) (2021) 499–509.
[51] Y. Dong, J.S. Pan, L. Zhang, Myostatin suppression of Akirin1 mediates glucocorticoid-induced satellite cell dysfunction, PLoS One 8 (3) (2013) e58554.
[52] O. Schakman, S. Kalista, C. Barbé, A. Loumaye, J.P. Thissen, Glucocorticoid-induced skeletal muscle atrophy, Int. J. Biochem. Cell Biol. 45 (10) (2013) 2163–2172.
[53] S. Lv, Q. Shen, H. Li, Q. Chen, W. Xie, Y. Li, X. Wang, G. Ding, Caloric restriction delays age-related muscle atrophy by inhibiting 11β-HSD1 to promote the differentiation of muscle stem cells, Front. Med. (Lausanne) 9 (2022) 1027055.
[54] S. Schluessel, W. Zhang, H. Nowotny, M. Bidlingmaier, S. Hintze, S. Kunz, S. Martini, S. Mehaffey, P. Meinke, C. Neuerburg, R. Schmidmaier, B. Schoser, N. Reisch, M. Drey, 11-beta-hydroxysteroid dehydrogenase type 1 (HSD11B1) gene expression in muscle is linked to reduced skeletal muscle index in sarcopenic patients, Aging Clin. Exp. Res. 35 (12) (2023) 3073–3083.
[55] I.V. Efimenko, D. Valancy, J.M. Dubin, R. Ramasamy, Adverse effects and potential benefits among selective androgen receptor modulators users: a cross-sectional survey, Int. J. Impot. Res. 34 (8) (2022) 757–761.
[56] M.R. Cho, S. Lee, S.K. Song, A Review of Sarcopenia Pathophysiology, Diagnosis, Treatment and Future Direction, J. Korean Med. Sci. 37 (18) (2022) e146.
[57] C. Gönen Aydın, A. Örsçelik, M.C. Gök, Y.E. Akman, The efficacy of extracorporeal shock wave therapy for chronic coccydynia, Med. Princ. Pract. 29 (5) (2020) 444–450.